Simultaneous Presence of Cationic and Reduced Gold in Functioning MgO-Supported CO Oxidation Catalysts: Evidence from X-ray Absorption Spectroscopy

Javier Guzman and Bruce C. Gates*

Department of Chemical Engineering and Materials Science, University of California, Davis, California 95616

Received: March 1, 2002; In Final Form: April 11, 2002

Gold clusters on the surface of MgO powder (calcined at 673 K) were prepared from adsorbed $[Au(CH_3)_2(acac)$, where acac is $C_5H_7O_2]$ and characterized by extended X-ray absorption fine structure (EXAFS) spectroscopy and X-ray absorption near edge spectroscopy (XANES). One sample initially contained gold predominantly in the form of clusters approximated as Au_6 on the basis of the EXAFS data showing first- and second-shell Au−Au coordination numbers of 4.0 ± 0.4 and 1.0 ± 0.1, respectively. The other sample initially contained larger clusters, with an average diameter of about 30 Å (containing about 100 atoms each, on average), as shown by the EXAFS first- and second-shell Au−Au coordination numbers of 9.4 ± 0.9 and 3.5 ± 0.4, respectively. The samples, in each of the three gases CO, O_2, and He and in the presence of CO + O_2 during CO oxidation catalysis, were investigated by EXAFS spectroscopy and XANES in a cell that was also a flow reactor. Data obtained during steady-state CO oxidation indicate the presence of gold clusters with an average diameter of about 30 Å, regardless of the initial size of the supported clusters. The XANES results demonstrate the simultaneous presence of both zerovalent and cationic gold in these catalysts.

Introduction

Supported gold clusters have been found to be surprisingly active catalysts for CO oxidation.[1−4] The unique properties have been variously attributed to the smallness of the clusters[5] and to the simultaneous presence of metallic gold atoms adjacent to cationic gold,[6,7] the latter suggested to be Au−OH groups on the basis of the effects of H_2 and of water in reactivating used catalysts.[6] However, it also has been suggested[7] that small metallic gold particles and not cationic gold species are responsible for the high steady-state catalytic activity for CO oxidation.

Expecting that the degree of oxidation and of aggregation of the gold might be dependent on the conditions of catalysis, our goal was to characterize the gold in a supported catalyst in the working state. We report an investigation of functioning MgO-supported gold clusters by X-ray absorption fine structure (EXAFS) spectroscopy and X-ray absorption near edge spectroscopy (XANES).

Experimental Section

Sample Synthesis. The syntheses and transfers of MgO-supported gold catalysts, described elsewhere,[8] were performed in the absence of moisture and air with a drybox (Braun MB-150M) purged with N_2 that was recirculated through traps containing particles of supported Cu and zeolite 4A for removal of O_2 and moisture, respectively. The catalysts, containing approximately 1 wt % Au, were prepared by slurrying $[Au(CH_3)_2(acac)]$ (Strem, 98%; acac is $C_5H_7O_2$) in dried and deoxygenated *n*-hexane (Aldrich, 99%) with MgO powder (EM Science, BET surface area 60 m^2/g)[9] that had been calcined in O_2 at 673 K. The slurry was stirred for 1 day and the solvent was removed by evacuation (pressure $<10^{-3}$ Torr) for 1 day. The resultant MgO-supported gold sample was treated in flowing He (Matheson, UHP grade; purified by passage through traps to remove traces of O_2 and moisture) at either 373 or 573 K.

CO Oxidation Catalysis. CO oxidation catalysis was carried out at atmospheric pressure and temperatures in the range of 298−573 K in either a standard once-through, nearly isothermal tubular packed-bed flow reactor (at the University of California) or in a flow-through X-ray absorption spectroscopy (XAS) cell[10] [at the Stanford Synchrotron Radiation Laboratory (SSRL)]. The catalyst (typically 0.05−0.30 g) was loaded into the reactor or the XAS cell in a drybox and transferred to a flow system without contacting air. Total feed flow rate to the flow system was 100 mL (NTP) min^{-1} with a CO partial pressure of 11 Torr and an O_2 partial pressure of 11 Torr and the remainder He. Each reactant, CO and O_2 (Matheson, UHP), each in a 10% mixture in He, was purified by passage through a trap containing activated γ-Al_2O_3 particles and zeolite 4A to remove any traces of metal carbonyls (from the high-pressure gas cylinder) and moisture, respectively. The conversions of CO and O_2 were determined by gas chromatographic analysis of the product stream, to determine the removal of CO and the formation of CO_2; the conversions were determined with an accuracy of about ±5%. The on-line gas chromatograph (Hewlett-Packard, HP-589 Series II) equipped for column switching in combination with two-channel detection[11] (with a thermal conductivity detector and a flame-ionization detector) was used to separate any possible water from other product gases on a polar column (Hayesep Q, 8 ft × $^1/_8$ in., 80−100 mesh), followed by separation of O_2, CO, and CO_2 in a zeolite 5A column (Chrompack, PLOT fused silica, 25 m × 0.53 mm). Transient conversion data during an initial induction period were determined for reaction at 373 K. Steady-state conversions following the induction period were measured at this and other temperatures in the range of 353−473 K.

In Situ X-ray Absorption Spectroscopy. XAS experiments were performed at beam lines 2-3 and 4-1 at SSRL. Data were

* To whom correspondence should be addressed.

10.1021/jp020584m CCC: $22.00
Published on Web 07/16/2002

recorded during CO oxidation catalysis and also with the catalysts in flowing He, CO, O_2, and in H_2 at atmospheric pressure and at a temperature of 373 K. Details of the sample handling are as presented elsewhere.[12] The synchrotron ring current was 50−100 mA, and the electron energy was 3 GeV. The double-crystal Si (220) monochromator was detuned by 20−25% at the Au L_{III} edge (11918.7 eV) to suppress higher harmonics in the X-ray beam. The reported data are the averages of seven scans (lasting approximately 17 min/scan), and no changes were detected between the first and the last scan, demonstrating that the synchrotron beam did not affect the supported gold.

Data Analysis

EXAFS. Analysis of the EXAFS data was carried out with a difference file technique with experimentally and theoretically determined reference files; details of the preparation of the reference files[13,14] and data analysis procedures are presented elsewhere.[12,15] The data were analyzed with the software XDAP.[16]

XANES. Quantitative interpretation of X-ray absorption near edge spectra remains challenging, even though the fundamental multiple-scattering (MS) theory of X-ray absorption is well established.[17−19] On one hand, the lack of self-consistent-field potentials and the large basis size requirements in existing MS codes makes them of limited accuracy; on the other hand, conventional ground-state electronic structure methods usually depend on lattice periodicity or neglect core-hole and self-energy effects.[19,20] Thus, only a qualitative interpretation of the XANES is reported.[21] The XANES data were calibrated with the simultaneously measured signal representing the Au L_{III} edge; this signal was determined with a gold foil in the beam path, scanned simultaneously with the sample. The edge is represented as the inflection point at the first absorption peak, at nearly 11 919 eV.[22] The data were normalized by dividing the absorption intensity by the height of the absorption edge.

Results

EXAFS Spectra of Catalysts Prior to Use. One catalyst (sample A), prepared from $[Au(CH_3)_2(acac)]$ adsorbed on MgO and subsequently treated in flowing He at 373 K for 2 h, initially contained gold predominantly in the form of extremely small clusters, modeled as Au_6 octahedra on the basis of the EXAFS data (Figure 1), showing first- and second-shell Au−Au coordination numbers of 4.0 ± 0.4 and 1.0 ± 0.1, respectively (Table 1).[8,23] The other catalyst (sample B), prepared from $[Au(CH_3)_2(acac)]$ adsorbed on MgO that had subsequently been treated in flowing He at 573 K for 2 h, initially contained larger (aggregated) clusters, with an average diameter of about 30 Å[24] (containing about 100 Au atoms each, on average),[25] as inferred from the EXAFS first- and second-shell Au−Au coordination numbers of 9.4 ± 0.9 and 3.5 ± 0.4, respectively (Table 1).

CO Oxidation Catalysis. The only observed product of the catalytic reaction was CO_2. Ignition behavior typical of CO oxidation was observed for each of the catalysts, as expected (data not shown).[2,4] The light-off temperature for each catalyst was approximately 390 K. The catalysts underwent deactivation in the flow reactor (e.g., Figure 2 shows the dependence of CO conversion on time on stream in the tubular flow reactor); after about 90 min, each catalyst attained a steady-state activity.

The initial activity of catalyst A was greater than that of catalyst B, but after about 40 min of operation, the activities of the two at 373 K became nearly the same (Figure 2). The activities approximately match those reported for other oxide-supported gold catalysts.[2] The data suggest the presence of essentially the same supported gold species in catalysts A and B after steady state had been attained.

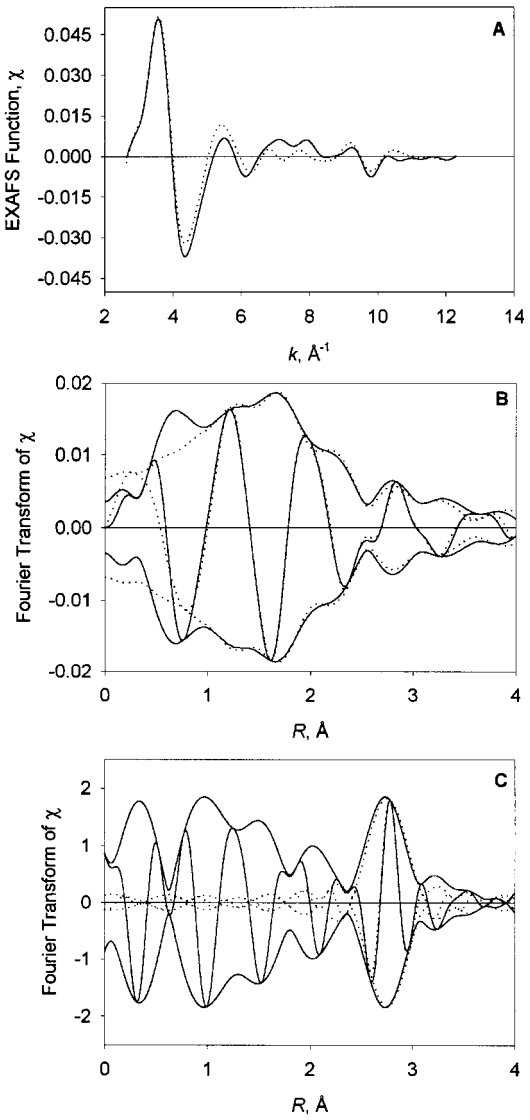

Figure 1. Results of EXAFS analysis characterizing the initially prepared sample A. (A) Experimental EXAFS function (solid line) and sum of the calculated Au−Au + $Au-O_s$ + $Au-O_l$ + Au−Mg contributions (dotted line). (B) Imaginary part and magnitude of uncorrected Fourier transform (k^0 weighted) of experimental EXAFS function (solid line) and sum of the calculated Au−Au + $Au-O_s$ + $Au-O_l$ + Au−Mg contributions (dotted line). (C) Residual spectrum illustrating the Au−Au contribution; imaginary part and magnitude of phase- and amplitude-corrected Fourier transform (k^0 weighted) of data minus the calculated $Au-O_s$ + $Au-O_l$ + Au−Mg contributions (solid line) and calculated Au−Au contribution (dotted line).

EXAFS Spectra of Catalysts in Various Atmospheres. EXAFS data were determined for each catalyst in the presence of each of the following gases: He, CO, O_2, and H_2. The results of the EXAFS analysis show the presence of Au−Au and Au−support interactions, the latter characterized by $Au-O_s$ and $Au-O_l$ contributions (where the subscripts s and l refer to short and long, respectively, consistent with the identification of the support as a multidentate oxygen-donor ligand).[26,27] Evidence of a weak contribution identified tentatively as Au−Mg was also found. The uncertainty of the assignment of the Au−Mg interaction makes the significance of the contribution unclear; the data do not allow a strong conclusion about this shell.[28]

TABLE 1: EXAFS Fit Parameters Characterizing MgO-Supported Gold Samples[a]

	sample A				sample B			
backscatterer	N	R (Å)	$10^3 \times \Delta\sigma^2$ (Å^2)	ΔE_0 (eV)	N	R (Å)	$10^3 \times \Delta\sigma^2$ (Å^2)	ΔE_0 (eV)
Au first shell	4.0	2.82	1.34	2.00	9.4	2.85	5.97	0.06
Au second shell	1.0	4.02	4.30	5.21	3.5	4.05	2.36	4.73
support O_s	1.2	2.16	4.24	5.73	1.1	2.17	5.91	6.41
support O_l	0.8	2.85	2.98	6.27	0.9	2.71	2.19	7.44
support Mg	0.9	2.73	1.26	2.54	0.9	2.72	2.91	0.53

[a] Notation: N, coordination number; R, distance between absorber and backscatterer atoms; $\Delta\sigma^2$, Debye−Waller factor; ΔE_0, inner potential correction. Expected errors: N, ±10%; R, ±0.02 Å; $\Delta\sigma^2$, ±20%; ΔE_0, ±20%. The subscripts s and l refer to short and long, respectively.

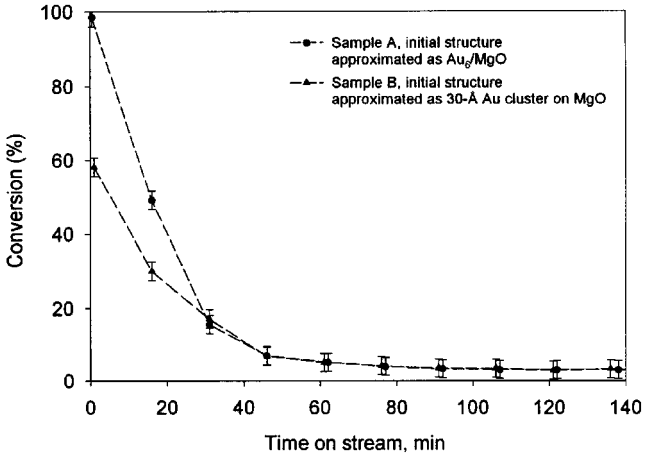

Figure 2. Oxidation of CO at 373 K in the presence of MgO-supported gold catalysts. Feed CO and O_2 partial pressures were 11 and 11 Torr, respectively; total feed flow rate was 100 mL·min^{-1} (NTP); mass of catalyst was 0.05 g.

Exposure of the initially prepared sample A to CO (P_{CO} = 11 Torr) or O_2 (P_{O_2} = 11 Torr) at 373 K led to the formation of gold clusters with average diameters of about 30 Å, as shown by the EXAFS first- and second-shell Au−Au coordination numbers of 9.5 ± 0.9 and 4.0 ± 0.5, respectively (Table 2). Exposure of sample A to H_2 (P_{H_2} = 760 Torr) at 373 K led to the formation of gold clusters smaller than those formed by treatment in CO or O_2, as shown by the EXAFS first- and second-shell Au−Au coordination numbers of 7.2 ± 0.7 and 3.5 ± 0.4, respectively (Table 2). Similar exposure of sample B (initially containing gold clusters about 30 Å in average diameter) to H_2, CO, or O_2 did not lead to significant changes in the average gold cluster size, as indicated by the Au−Au first- and second-shell coordination numbers (data not shown).

The Au−O and Au−Mg contributions in the EXAFS spectra of samples A and B determine coordination numbers and distances (Table 1) that are typical of noble metals supported on metal oxides.[29] The Au−O contribution characterizing sample A after exposure to O_2 was greater than that of the sample initially in the presence of He, H_2, or CO (Table 2), consistent with some oxidation of the gold by O_2. The EXAFS data representing sample A in O_2 include one relatively long Au−O contribution (Au−O_l; coordination number N = 2.5, distance R = 2.70 Å) and another, shorter contribution, Au−O_s (N = 2.4, R = 2.17 Å); this latter Au−O distance corresponds to a bonding distance.[28,29]

XANES Data. XANES provides information about the oxidation states and site symmetries of the gold species.[17,20] XANES peak locations and intensities for reference materials containing gold in various oxidation states are summarized in Table 3. Data for Au(0) were measured with gold foil, data for Au(I) with crystalline AuCl and [(PPh_3)AuCl], and data for Au(III) with crystalline [$Au(CH_3)_2$(acac)] (in a mixture with boron nitride). These and related data of Table 3 provide a basis for interpretation of the features in the XANES of our supported gold samples.

Data characterizing the reference materials show that there is a prominent feature in the Au L_{III} near-edge spectra of Au(III) centered at an energy 4 eV above the X-ray absorption edge. This absorption peak is missing from the spectra of metallic gold because of the complete occupancy of the d states (gold ground-state electron configuration [Xe]$4f^{14}5d^{10}6s^1$).[30,31] Furthermore, the spectrum of Au(III) shows a shoulder at an energy 15 eV and a broad shoulder at 50 eV above the X-ray absorption edge, whereas the spectrum of Au(0) shows a shoulder at 15 eV and intense peaks at 25 and 50 eV above the edge. Similarly, XANES characterizing Au(I) have been observed to include a peak of intermediate intensity with respect to that of Au(III) and Au(0) at 4 eV above the edge.[31,32] The spectrum of Au(I) also includes a shoulder at 15 eV and strong peaks at 25 and 50 eV higher than the edge.

XANES of our samples treated in O_2 clearly indicate Au(III), identified by the intense peak at 4 eV, a shoulder at 15 eV, and a broad shoulder at 50 eV above the X-ray absorption edge (Table 3, Figure 3). Data representing the samples treated in H_2 provide evidence of metallic gold, as evident from the absence of a peak at 4 eV and the presence of a shoulder at 15 eV and intense peaks at 25 and 50 eV higher than the edge.

XANES characterizing the initially prepared sample A, represented as Au_6/MgO (treated in He; Figure 3A), include an intense peak at 4 eV, a shoulder at 15 eV, and a broad shoulder at 50 eV higher than the edge. These peaks and their intensities match the features characterizing Au(III) (Table 3, Figure 3) (even after seven scans with the X-ray beam). Exposure of this sample to H_2 at 373 K led to the complete disappearance of the peak at 4 eV and to the appearance of an intense peak at 25 eV above the edge, and the peak at 50 eV above the edge became narrower (Figure 3E), indicating reduction and formation of metallic gold. The XANES characterizing the supported species formed after exposure of the initial sample A to O_2 (P_{O_2} = 11 Torr) at 373 K (Figure 3B) show features similar to those observed for the supported sample as initially prepared from [$Au(CH_3)_2$(acac)], indicating cationic gold. Exposure of the initially prepared sample A to CO (P_{CO} = 11 Torr) at 373 K (Figure 3C) resulted in a decrease in intensity of the peak at 4 eV and the appearance of an intense peak at 25 eV above the edge. The data demonstrate reduction of the gold to an intermediate oxidation state; a comparison of the spectrum with those of AuCl and [(PPh_3)AuCl] and with that of metallic gold (Table 3, Figure 3) indicates the presence of both Au(I) and Au(0).

X-ray Absorption Spectra of Functioning CO Oxidation Catalysts. EXAFS spectra show that, after exposure of either initially prepared catalyst to a reacting mixture of CO and O_2 (P_{CO} = 11 Torr and P_{O_2} = 11 Torr) after attainment of steady state at 373 K[33] (Figure 4), the predominant supported species in the functioning catalysts were gold clusters with an average diameter of about 30 Å, as indicated by the first-shell Au−Au coordination number of 10 ± 1 (with a bond distance of 2.86 ± 0.02 Å) and the second-shell Au−Au coordination number of 4.5 ± 0.4 (at a distance of 4.05 ± 0.04 Å) (Table 4). The EXAFS data are consistent with the catalytic data indicating the presence of essentially the same supported gold species in

TABLE 2: EXAFS Results Characterizing Sample A in H_2, O_2, and CO at 373 K and a Pressure of 760 Torr[a]

	treatment gas											
	H_2				O_2				CO			
backscatterer	N	R (Å)	$10^3 \times \Delta\sigma^2$ (Å^2)	ΔE_0 (eV)	N	R (Å)	$10^3 \times \Delta\sigma^2$ (Å^2)	ΔE_0 (eV)	N	R (Å)	$10^3 \times \Delta\sigma^2$ (Å^2)	ΔE_0 (eV)
Au first shell	7.2	2.79	8.54	1.60	10.4	2.84	8.50	1.87	9.2	2.85	4.52	1.54
Au second shell	3.5	3.85	8.21	9.78	3.1	4.05	3.98	10.44	4.0	4.05	6.23	3.31
support O_s	1.1	2.14	6.69	2.55	2.4	2.17	6.63	0.33	1.0	2.16	5.72	2.63
support O_l	0.8	2.83	5.33	1.42	2.5	2.70	8.74	5.35	0.8	2.75	4.75	2.32
support Mg	0.8	2.72	6.42	1.35	0.8	2.73	5.47	1.63	0.9	2.71	6.51	1.27

[a] Notation as in Table 1.

TABLE 3: XANES Features Characterizing Supported Gold Samples and Reference Materials

sample	treatment gas	peak positions[a] (eV)	Au oxidation state(s)	ref
		Reference Material		
Au foil	none	15 sh, 25 vs, 50 s[b]	0	32
Au_2Cl_6	none	4 vs, 15 s, 50 sh[b]	+3	32
AuCl	none	4 s, 15 sh, 25 s, 50 sh[b]	+1	32
Au foil	none	15 sh, 27 vs, 49 s	0	31
$KAuCl_4$	none	4 vs, 15 s, 49 sh	+3	31
$(PPh_3)AuCl$	none	4 s, 27 s, 49 sh	+1	31
$[Au(CH_3)_2(acac)]/BN$	none	4 vs, 15 sh, 50 s	+3	this work
Au foil	none	15 sh, 25 vs, 50 s	0	this work
		Catalyst		
A	He	4 vs, 15 sh, 50 sh	+3[c]	this work
B	He	15 sh, 25 vs, 50 s	0[c]	this work
A or B	H_2	15 sh, 25 vs, 50 s	0[c]	this work
A or B	O_2	4 vs, 15 sh, 50 sh	+3[c]	this work
A or B	CO	4 s, 15 sh, 25 s, 50 sh	0 and +1[c]	this work
A or B	$CO + O_2 + He$	4 s, 15 sh, 25 s, 50 sh	0 and +1[c]	this work

[a] Above the X-ray Au L_{III} absorption edge; vs, very strong; s, strong; sh, shoulder. [b] Approximated values from reference. [c] Tentative assignment on the basis of comparison between the data and reference materials.

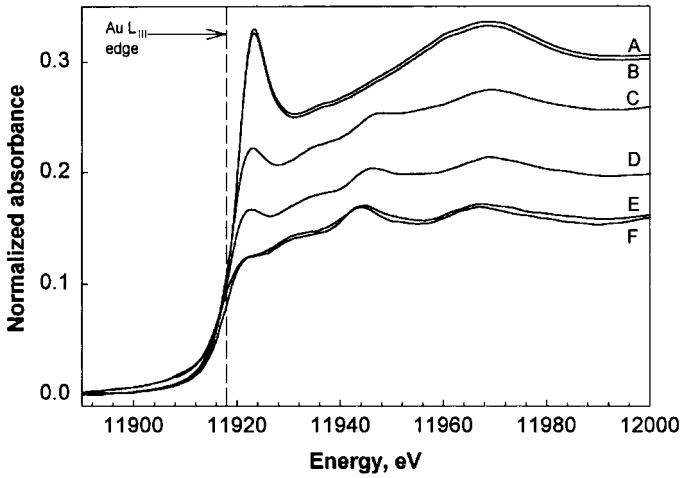

Figure 3. XANES characterizing MgO-supported gold clusters scanned after (A) adsorption of $[Au(CH_3)_2(acac)]$ followed by treatment in He at 373 K and subsequent exposure to the following atmospheres: (B) O_2 at 373 K, (C) CO at 373 K, (D) CO and O_2 at 373 K, and (E) H_2 at 373 K. (F) XANES characterizing gold foil. The theoretical energy of the Au L_{III} edge (vertical dashed line) is given relative to the Fermi level of the metal.

each catalyst after attainment of steady state, regardless of the initial structure of the supported gold (Table 4).

The XANES show that after exposure of the initially prepared catalyst A to a reacting mixture of CO and O_2 ($P_{CO} = 11$ Torr and $P_{O_2} = 11$ Torr, Figure 3D) after attainment of steady state at 373 K, cationic gold, approximated as Au(I), and zerovalent gold were formed simultaneously. This conclusion is drawn on the basis of (a) the simultaneous reduction in intensity, without disappearance, of the peak at 4 eV higher than the edge and (b) the appearance of a peak at 25 eV above the X-ray absorption edge accompanied by the change in intensities of the peaks at 15 and 50 eV higher than the edge, characteristic of cationic and metallic gold, respectively.

Consistent with these conclusions, the EXAFS data indicate that treatment in O_2 increases the Au−O coordination numbers (for Au−O_l, $N = 2.5$ and $R = 2.70$ Å; for Au−O_s, $N = 2.4$ and $R = 2.17$ Å), suggesting oxidation of the clusters and indicating the presence of oxygen in the vicinity of gold. In contrast, during steady-state catalysis in CO and O_2, these coordination numbers (for Au−O_l, $N = 0.9$ and $R = 2.75$ Å; for Au−O_s, $N = 0.9$ and $R = 2.17$ Å) are less, suggesting that there is less oxygen bonded to the gold during catalysis than in the presence of O_2 alone,

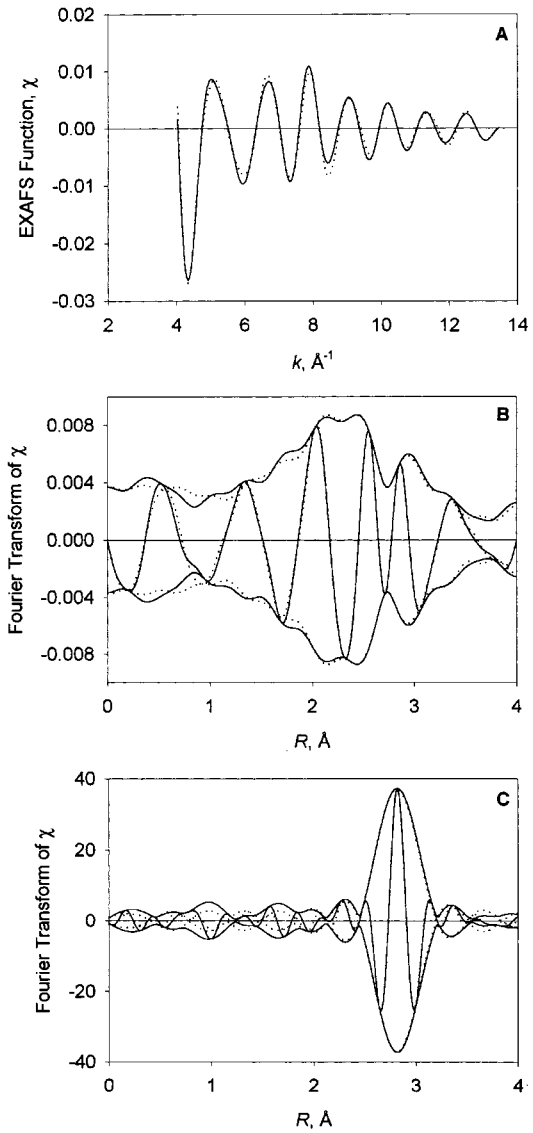

Figure 4. Results of EXAFS analysis characterizing the supported species in the functioning catalyst (initially prepared as sample A) after exposure to a reactant mixture of CO and O_2 (P_{CO} = 11 Torr and P_{O_2} = 11 Torr) after attainment of steady state at 373 K. (A) Experimental EXAFS function (solid line) and sum of the calculated Au−Au + Au−O_s + Au−O_l + Au−Mg contributions (dotted line). (B) Imaginary part and magnitude of uncorrected Fourier transform (k^0 weighted) of experimental EXAFS function (solid line) and sum of the calculated Au−Au + Au−O_s + Au−O_l + Au−Mg contributions (dotted line). (C) Residual spectrum illustrating the Au−Au contribution; imaginary part and magnitude of phase- and amplitude-corrected Fourier transform (k^0 weighted) of data minus the calculated Au−O_s + Au−O_l + Au−Mg contributions (solid line) and calculated Au−Au contribution (dotted line).

consistent with the reaction of some of the gold with CO, as would be expected from the occurrence of catalysis.

Discussion

Aggregation of Gold Clusters on Partially Hydroxylated MgO Surfaces. Treatment of sample A (containing predominantly clusters approximated as Au_6) in H_2, O_2, or CO at 373 K led to aggregation of the gold. Thus, we infer that the initially supported gold species migrated readily on the MgO surface. Similarly, the aggregation of metal clusters on MgO during H_2 or O_2 treatment at various temperatures has been demonstrated for clusters approximated as Ir_4[34−36] and Ir_6.[37,38] Comparable results have been observed, for example, for Ir_4 and Ir_6 on La_2O_3,[39] Rh_6 and Ir_4 on TiO_2,[40,41] Os_5C on MgO,[42,43] and Rh_6 on MgO.[44,45] It has been suggested[34,38] that the density of hydroxyl groups on the MgO influences the aggregation of the supported metal clusters, possibly by affecting the strength of the metal−support interaction. The results suggest that the hydroxyl groups on our MgO support, which was calcined at 673 K and had almost 50% of its surface covered by OH groups,[46−49] facilitates the aggregation of the gold clusters.

TABLE 4: EXAFS Results Characterizing MgO-Supported Gold Species during CO Oxidation Catalysis at 373 K and 760 Torr[a,b]

	initially prepared MgO-supported gold species							
	sample A				sample B			
backscatterer	*N*	*R* (Å)	$10^3 \times \Delta\sigma^2$ (Å^2)	ΔE_0 (eV)	*N*	*R* (Å)	$10^3 \times \Delta\sigma^2$ (Å^2)	ΔE_0 (eV)
Au first shell	10.0	2.86	4.31	1.23	9.5	2.84	6.87	1.02
Au second shell	4.5	4.05	3.53	4.12	4.2	4.06	3.90	9.38
support O_s	0.9	2.17	2.14	2.43	0.8	2.17	1.42	5.24
support O_l	0.9	2.75	6.42	5.62	0.7	2.79	2.36	6.66
support Mg	0.6	2.72	8.87	1.36	0.6	2.72	3.98	2.01

[a] Notation as in Table 1. [b] Data were obtained during steady-state catalysis following an induction period in the flow reactor cell.

Evidence of Gold in Various Oxidation States. The XANES characterizing sample A, formed by adsorption of [$Au(CH_3)_2$(acac)] on MgO and followed by treatment in He at 373 K for 2 h, is similar to that of crystalline [$Au(CH_3)_2$(acac)], which contains Au(III).[50−52] This comparison suggests that the gold, at least in part, retained its oxidation state after adsorption of the precursor (and the results show that it was stable in the X-ray beam). The XANES of sample A recorded after it had been treated in H_2 at 373 K is nearly identical to that of gold foil. Thus, we conclude that H_2 treatment led to essentially complete reduction of the Au(III) that was originally present in sample A, to give Au(0). Our results agree with previous reports[2,53] showing the reduction of supported gold to the metallic state as a result of H_2 treatment.

The XANES of sample B, formed by adsorption of [$Au(CH_3)_2$(acac)] on MgO followed by treatment in He at 573 K for 2 h (which initially contained aggregated clusters with an average diameter of about 30 Å), is similar to that of sample A after it had been treated in H_2 at 373 K; the spectra essentially match that of gold foil. Thus, we infer that sample B contained predominantly Au(0). These results agree with a previous report[8] of the decrease in gold oxidation state with increasing temperature of treatment in He, as the CH_3 and acac groups are removed from the coordination sphere of the metal in the species formed from [$Au(CH_3)_2$(acac)].

Simultaneous Presence of Au(III) and Au(0) in Functioning MgO-Supported CO Oxidation Catalysts. Oh et al.,[6] on the basis of data characterizing deactivation and reactivation of used catalysts, suggested a mechanism for catalytic oxidation of CO via the formation and decomposition of surface formate and bicarbonate and active sites, each consisting of an ensemble of a gold−hydroxyl group and metallic gold atoms. In contrast, Haruta and Daté[7] suggested that metallic gold particles and not cationic gold are responsible for the high steady-state catalytic activity. Moreover, they suggested that the support and the interface at the perimeters of gold particles play a major role in the CO oxidation reaction.

Our data show that once the CO oxidation reaction had attained steady state, the gold had aggregated into clusters with an average diameter of about 30 Å. Furthermore, our XANES

data characterizing the functioning catalysts indicate the simultaneous presence of a mixture of cationic and metallic gold. On one hand, the intensity of the peak at 4 eV higher than the absorption edge in the XANES—relative to those of the same peak in the spectra of Au(III) and Au(0)—suggests the presence of gold in an intermediate oxidation state, likely Au(I). Gold in oxidation state +1 is only slightly less stable than Au(III).[2,32,53,54] On the other hand, the appearance of peaks at 15 and 25 eV above the X-ray absorption edge is characteristic of metallic gold, as illustrated by the XANES of gold foil (Figure 3F). Because the spectra of the functioning catalysts do not show a complete disappearance of the peak at 4 eV higher than the edge, as would be expected for metallic gold alone, we infer the presence of both Au(I) and Au(0) in the functioning catalysts.

This conclusion is consistent with the interpretation of Oh et al.[6] suggesting the simultaneous presence of cationic and metallic gold in the catalytically active species in CO oxidation. Furthermore, the conclusion is consistent with the mechanism proposed by Haruta and Daté[7] for CO oxidation on Au/TiO_2 catalysts, according to which either molecular oxygen or atomic oxygen is adsorbed on cationic gold at the perimeters of the metallic gold clusters.

Oh et al.[6] attributed the deactivation of their catalysts to dehydroxylation of the surface associated with gold cations and to formation of carbonate, and not to sintering of the metal. The deactivation of our catalyst B might be interpreted similarly, but the greater deactivation of our catalyst A suggests a combination of sintering (which was demonstrated by the EXAFS data) and the dehydroxylation and/or carbonate formation.

Postulate: Ensembles of Au(I) and Au(0) in MgO-Supported Gold Catalysts. Although the XANES demonstrate the simultaneous presence of Au(I) and Au(0) in the catalysts, these data do not provide a basis for distinguishing between an ensemble of cationic and zerovalent gold and a mixture of two segregated phases, one containing Au(I) and the other Au(0). There is precedent for the former type of structure, illustrated by highly dispersed Pt—W catalysts supported on γ-Al_2O_3.[55] In these samples, the oxophilic tungsten cations evidently bond both to the oxide support and to the noble metal clusters, helping to maintain the high dispersion and stability of the latter.[55] Furthermore, the interactions of tungsten cations with platinum decreases both the chemisorption capacity of the platinum clusters for H_2 and CO and the catalytic activity for toluene hydrogenation. We postulate the occurrence of similar structures in our catalysts, consistent with an earlier speculation.[56] In such a structure, the arrangement of cationic and zerovalent gold in the supported structures would be expected to influence the chemisorption and catalytic properties of the material.

Conclusions

The simultaneous presence of Au(I) and zerovalent gold clusters with an average diameter of about 30 Å in MgO-supported catalysts was demonstrated by XANES of the functioning catalysts during steady-state CO oxidation. The initial dispersion and oxidation state of the gold in the catalyst were found not to affect the properties of the catalysts functioning at steady state. The data are consistent with the postulate that the catalytically active species consist of zerovalent gold clusters interacting with cationic gold at the cluster—support interface.

Acknowledgment. This research was supported by the U.S. Department of Energy, Office of Energy Research, Office of Basic Energy Sciences, Division of Chemical Sciences, Contract FG02-87ER13790. We acknowledge the Stanford Synchrotron Radiation Laboratory (SSRL), which is operated by Stanford University for the U.S. Department of Energy, Office of Basic Energy Science, for access to beam time on beam lines 2-3 and 4-1. We thank the staff of the SSRL for their assistance. The X-ray absorption data were analyzed with the XDAP software.[16]

References and Notes

(1) Haruta, M.; Tsubota, S.; Kobayashi, T.; Kageyama, H.; Genet, M. J.; Delmon, B. *J. Catal.* **1993**, *144*, 175.
(2) Bond, G. C.; Thompson, D. T. *Catal. Rev.-Sci. Eng.* **1999**, *41*, 319.
(3) Kozlov, A. I.; Kozlova, A. P.; Liu, H.; Iwasawa, Y. *Appl. Catal. A* **1999**, *182*, 9.
(4) Haruta, M. *Catal. Today* **1997**, *36*, 153.
(5) Heiz, U.; Schneider, W.-D. *J. Phys. D* **2000**, *33*, R85.
(6) Oh, H.-S.; Costello, C. K.; Cheung, C.; Kung, H. H.; Kung, M. C. *Stud. Surf. Sci. Catal.* **2001**, *139*, 375.
(7) Haruta, M.; Daté, M. *Appl. Catal. A* **2001**, *222*, 427.
(8) Guzman, J.; Gates, B. C. *Nano Lett.* **2001**, *1*, 689.
(9) Panjabi, G.; Argo, A. M.; Gates, B. C. *Chem. Eur. J.* **1999**, *5*, 2417.
(10) Odzak, J. F.; Argo, A. M.; Lai, F. S.; Gates, B. C.; Pandya, K.; Feraria, L. *Rev. Sci. Instrum.* **2001**, *72*, 3943.
(11) Lai, F. S.; Gates, B. C. *Nano Lett.* **2001**, *1*, 583.
(12) Kirlin, P. S.; van Zon, F. B. M.; Koningsberger, D. C.; Gates, B. C. *J. Phys. Chem.* **1990**, *94*, 8439.
(13) van Zon, J. B. A. D.; Koningsberger, D. C.; van't Blik, H. F. J.; Sayers, D. E. *J. Chem. Phys.* **1985**, *82*, 5742.
(14) Duivenvoorden, F. B. M.; Koningsberger, D. C.; Uh, Y. S.; Gates, B. C. *J. Am. Chem. Soc.* **1986**, *108*, 6254.
(15) Weber, W. A.; Gates, B. C. *J. Phys. Chem. B* **1997**, *101*, 10423.
(16) Vaarkamp, M.; Linders, J. C.; Koningsberger, D. C. *Physica B* **1995**, *209*, 159.
(17) Bianconi, A. In *X-ray Absorption, Principles, Applications, Techniques of EXAFS, SEXAFS and XANES*; Koningsberger, D. C., Prins, R., Eds.; Wiley: New York, 1988; Chapter 11.
(18) Lloyd, P.; Smith, P. V. *Adv. Phys.* **1972**, *21*, 69.
(19) Ankudinov, A. L.; Ravel, B.; Rehr, J. J.; Conradson, S. D. *Phys. Rev. B* **1998**, *58*, 7565.
(20) Rehr, J. J.; Albers, R. C. *Rev. Mod. Phys.* **2000**, *72*, 621.
(21) The absorption peak nearest the absorption edge, centered at an energy 4 eV above the edge, is sometimes called the white line. Measurements of the area under the white line have sometimes been reported, but these are no longer considered to be significant.
(22) The shift in the absorption edge is not reported, because the measured shifts are influenced by the movement of the monochromator and by the step size during scanning.
(23) The postulated model consisting of octahedral Au_6 clusters is simplified; we do not exclude the possible presence of other clusters in the sample.
(24) Kip, B. J.; Duivenvoorden, F. B. M.; Koningsberger, D. C.; Prins, R. *J. Catal.* **1987**, *105*, 26.
(25) Jentys, A. *Phys. Chem. Chem. Phys.* **1999**, *1*, 4059.
(26) Alexeev, O.; Gates, B. C. *Top. Catal.* **2000**, *10*, 273.
(27) Gates, B. C. *J. Mol. Catal. A* **2000**, *163*, 55.
(28) Goellner, J. F.; Gates, B. C.; Vayssilov, G. N.; Rösch, N. *J. Am. Chem. Soc.* **2000**, *122*, 8056.
(29) Gates, B. C. *Top. Catal.* **2001**, *14*, 173.
(30) Hammer, B.; Nørskov, J. K. *Nature* **1995**, *376*, 238.
(31) Benfiled, R. E.; Grandjean, D.; Kröll, M.; Pugin, R.; Sawitowski, T.; Schmid, G. *J. Phys. Chem. B* **2001**, *105*, 1961.
(32) Salama, T. M.; Shido, T.; Ohnishi, R.; Ichikawa, M. *J. Phys. Chem.* **1996**, *100*, 3688.
(33) The conversion expected in the flow reactor/XAS cell on the basis of data obtained with the tubular packed-bed flow reactor was about 3%.
(34) Triantafillou, N. D.; Gates, B. C. *J. Phys. Chem.* **1994**, *98*, 8431.
(35) Xiao, F.-S.; Xu, Z.; Alexeev, O.; Gates, B. C. *J. Phys. Chem.* **1995**, *99*, 1548.
(36) Alexeev, O.; Kim, D.-W.; Gates, B. C. *J. Mol. Catal. A* **2000**, *162*, 67.
(37) Maloney, S. D.; Kelly, M. J.; Koningsberger, D. C. Gates, B. C. *J. Phys. Chem.* **1991**, *95*, 9406.
(38) Kawi, S.; Gates, B. C. *Inorg. Chem.* **1992**, *31*, 2939.
(39) Triantafillou, N. D.; Gates, B. C. *Langmuir* **1999**, *15*, 2595.
(40) Goellner, J. F.; Gates, B. C. *J. Phys. Chem. B* **2001**, *105*, 3269.
(41) Goellner, J. F.; Guzman, J.; Gates, B. C. *J. Phys. Chem. B* **2002**, *106*, 1229.
(42) Lamb, H. H.; Fung, A. S.; Tooley, P. A.; Puga, J.; Krause, T. R.; Kelley, M. J.; Gates, B. C. *J. Am. Chem. Soc.* **1989**, *111*, 8367.
(43) Allard, L. F.; Panjabi, G. A.; Salvi, S. N.; Gates, B. C. *Nano Lett.* **2002**, *2*, 381.

(44) Weber, W. A. Ph.D. Dissertation, University of California, Davis, 1998.
(45) Argo, A. M. Ph.D. Dissertation, University of California, Davis, 2001.
(46) Lamb, H. H.; Gates, B. C.; Knözinger, H. *Angew. Chem., Int. Ed. Engl.* **1988**, *27*, 1127.
(47) Lamb, H. H.; Gates, B. C. *J. Am. Chem. Soc.* **1986**, *108*, 81.
(48) Papile, C. J.; Gates, B. C. *Langmuir* **1992**, *8*, 74.
(49) van Zon, F. B. M.; Maloney, S. D.; Gates, B. C.; Koningsberger, D. C. *J. Am. Chem. Soc.* **1993**, *115*, 10317.
(50) Miles, M. G.; Glass, G. E.; Tobias, R. S. *J. Am. Chem. Soc.* **1966**, *88*, 5738.
(51) Kuch, P. L.; Tobias, R. S. *J. Organomet. Chem.* **1976**, *122*, 429.
(52) Shibata, S.; Iijima, K.; Baum, T. H. *J. Chem. Soc., Dalton Trans.* **1990**, *4*, 1519.
(53) Galvagno, S.; Parravano, G. *J. Catal.* **1978**, *55*, 178.
(54) Bassi, I. W.; Lytle, F. W.; Parravano, G. *J. Catal.* **1976**, *42*, 139.
(55) Alexeev, O.; Graham, G. W.; Shelef, M.; Gates, B. C. *J. Catal.* **2000**, *190*, 157.
(56) Bond, G. C.; Thompson, D. T. *Gold Bull.* **2000**, *33*, 41.